Biosensors and Bioelectronics 126 (2019) 510–517

Contents lists available at ScienceDirect

Biosensors and Bioelectronics

journal homepage: www.elsevier.com/locate/bios

Surface regeneration and reusability of label-free DNA biosensors based on weak polyelectrolyte-modified capacitive field-effect structures

Thomas S. Bronder[a,b], Arshak Poghossian[a,c,*], Max P. Jessing[a], Michael Keusgen[b], Michael J. Schöning[a,c,*]

[a] Institute of Nano- and Biotechnologies, FH Aachen, Campus Jülich, 52428 Jülich, Germany
[b] Institute of Pharmaceutical Chemistry, Philipps University Marburg, 35037 Marburg, Germany
[c] Institute of Complex Systems Bioelectronics (ICS-8), Forschungszentrum Jülich GmbH, 52425 Jülich, Germany

ARTICLE INFO

Keywords:
DNA biosensor
Label-free
Field-effect sensor
Reusability
Weak polyelectrolyte
Charge screening

ABSTRACT

The reusability of capacitive field-effect electrolyte-insulator-semiconductor (EIS) sensors modified with a cationic weak polyelectrolyte (poly(allylamine hydrochloride) (PAH)) for the label-free electrical detection of single-stranded DNA (ssDNA), in-solution- and on-chip-hybridized double-stranded DNA (dsDNA) has been studied. It has been demonstrated that via simply regeneration of the gate surface of the EIS sensor by means of an electrostatic adsorption of a new PAH layer, the same biosensor can be reused for at least five DNA-detection measurements. Because of the reversal of the charge sign of the outermost layer after each surface modification with the cationic PAH or negatively charged DNA molecules, the EIS-biosensor signal exhibits a zigzag-like behavior. The amplitude of the signal changes has a tendency to decrease with increasing number of macromolecular layers. The direction of the EIS-signal shifts can serve as an indicator for a successful DNA-immobilization or -hybridization process. In addition, we observed that the EIS-signal changes induced by each surface-modification step (PAH adsorption, immobilization of ssDNA or dsDNA molecules and on-chip hybridization of complementary target cDNA) is decreased with increasing the ionic strength of the measurement solution, due to the more efficient macromolecular charge-screening by counter ions. The results of field-effect experiments were supported by fluorescence-intensity measurements of the PAH- or DNA-modified EIS surface using various fluorescence dyes.

1. Introduction

Deoxyribonucleic acid (DNA) sensors have been widely recognized as a powerful tool in many fields of application such as molecular diagnostics, forensics, parental testing, drug industry, food safety, identification of pathogens, environmental monitoring of biological warfare and bioterrorism agents, etc. (Wei et al., 2010; Sassolas et al., 2008; Zhao et al., 2014). Among different transducers suggested for label-free DNA detection, an electrolyte-gated field-effect device (FED) based on an electrolyte-insulator-semiconductor (EIS) system is one of the most popular and attractive platforms (Poghossian and Schöning, 2014; Kataoka-Hamai and Miyahara, 2011; Veigas et al., 2015; Toumazou et al., 2014). FEDs offer a lot of advantages, like small sizes, the possibility of real-time measurements, fast response and large-scale production at low cost by using of advanced nano- and microfabrication technologies, thus providing new opportunities for a next generation of label-free DNA chips with direct electronic readout.

FEDs are surface charge-sensitive devices and have been widely applied for the detection of various analytes in liquids, including charged macromolecules such as DNA or polyelectrolytes (see e.g., Poghossian et al., 2001; Gun et al., 2008; Jimenez-Jorquera et al., 2010; Poghossian et al., 2000; Siqueira et al., 2009; Nakazato, 2009; Lee et al., 2009, Poghossian et al., 2015). Most of FED-based DNA biosensors reported in literature rely on DNA-hybridization detection (see e.g., Lu et al., 2013; Wu et al., 2014; Bandiera et al., 2007; Ingebrandt and Offenhäusser, 2006), although detection of other DNA-recognition events, like single-nucleotide polymorphisms (Purushothaman et al., 2006; Ingebrandt et al., 2007), DNA extension (Kamahori et al., 2008) and sequencing (Rothberg et al., 2011), DNA amplification by polymerase chain reaction (PCR) (Goda et al., 2015; Toumazou et al., 2013; Salm et al., 2014), by-products (protons, pyrophosphates) of the nucleotide base incorporation reaction (Veigas et al., 2014; Credo et al., 2012), have also been proposed. In DNA-hybridization reaction, the probe single-stranded DNA (ssDNA) molecules of known sequence bind

* Corresponding authors at: Institute of Nano, and Biotechnologies, FH Aachen, Campus Jülich, 52428 Jülich, Germany.
E-mail addresses: a.poghossian@fz-juelich.de (A. Poghossian), schoening@fh-aachen.de (M.J. Schöning).

https://doi.org/10.1016/j.bios.2018.11.019
Received 20 September 2018; Received in revised form 5 November 2018; Accepted 13 November 2018
Available online 15 November 2018
0956-5663/

specifically to their complementary single-stranded target DNA (cDNA) and forming a double-stranded DNA (dsDNA). Typically, capture-probe ssDNA molecules are immobilized onto the gate surface of the FED chip and the target cDNA molecules are either detected by real-time monitoring the FED response directly during the hybridization process or by comparing the biosensor signal before and after hybridization. FEDs detect DNA molecules electrostatically by their intrinsic negative molecular charge that arises from the phosphate backbones. The adsorption/binding of charged DNA to the gate surface of the FED modulates the space-charge distribution in the semiconductor, resulting in a change of the output signal of the FED (Poghossian and Schöning, 2014; Kataoka-Hamai and Miyahara, 2011; Veigas et al., 2015). Generally, due to the screening of the DNA molecular charge by counterions in the solution, the effectivity of an electrostatic coupling between the charged DNA and the FED and therefore, the magnitude of the DNA-hybridization signal is significantly affected by the Debye length or ionic strength of the electrolyte solution, by the distance between the gate surface and molecular charge and by the orientation of DNA macromolecules to the gate surface (Poghossian et al., 2005; Liu and Dutton, 2009; Zhang et al., 2008; Nishio et al., 2013; Lai et al., 2015). Thus, among others the gate surface-modification/functionalization and DNA-immobilization technique have a significant impact on the FED signal generated by the DNA hybridization. As a consequence, in addition to recording the DNA-hybridization signal in a low ionic-strength solution, the immobilization of DNA molecules flat to the FED surface with molecular charge lying within the Debye length from the gate surface represents a crucial factor to enhance the sensitivity of the FED to the DNA charge (Braeken et al., 2008). One approach to achieve flat orientation of DNA molecules on the surfaces is the layer-by-layer (LbL) electrostatic adsorption of a cationic polyelectrolyte/DNA bilayer (Evtugyn and Hianik, 2011), which has also been used for designing FED-based DNA biosensors. For example, poly-L-lysine-modified ion-sensitive field-effect transistors and EIS sensors were utilized for the detection of ssDNA- and dsDNA-immobilization, DNA-hybridization process (Braeken et al., 2008; Fritz et al., 2002; Lin et al., 2010) as well as for monitoring PCR-amplified dsDNA (Hou et al., 2006, 2007).

Recently, in our group, the feasibility for the label-free electrical detection of DNA with two kinds of FEDs, the capacitive EIS sensor and multi-spot light-addressable potentiometric sensor (LAPS), which were modified with a positively-charged weak polyelectrolyte of poly(allylamine hydrochloride) (PAH), has been demonstrated (Bronder et al., 2015, 2017; Wu et al., 2015, 2016). The capacitive EIS and LAPS devices modified with a PAH layer demonstrate high DNA-hybridization signals (several tens of mVs) and low detection limits (about 0.1–0.3 nM cDNA). Moreover, PAH-modified EIS sensors were applied for the detection of PCR-amplified tuberculosis DNA fragments and could be applied for a quick verification of the DNA amplification and successful PCR process (Poghossian et al., 2016; Bronder et al., 2018).

DNA biosensors are often designed as disposables for a single-use measurement. To make DNA biosensors reusable, the complex surface/interface architecture should be regenerated after it has been used. This is often realized by removing DNA molecules together with underlying linkers or molecular layers from the sensor's surface and modification of the surface for DNA coupling again, which is a complicated and time-consuming process in many cases (see e.g., a review on common techniques of biosensor regeneration (Goode et al., 2015)). In the present work, the possibility of a multiple surface regeneration and reusability of PAH-modified EIS sensors for the label-free electrostatic detection of i) ssDNA, ii) in-solution hybridized dsDNA, and iii) on-chip hybridization of complementary target cDNA with immobilized probe ssDNA is investigated. In addition, impact of the ionic strength and charge screening on the EIS sensor signal has been examined. Fluorescence microscopy measurements by using fluorescence dyes of FITC (fluorescein isothiocyanate), FAM (carboxyfluorescein) and SG (Sybr-Green I) have been performed to validate the results of field-effect experiments.

2. Materials and methods

2.1. Materials and solutions

Polyelectrolyte solutions were prepared by solving PAH (Mw: 100.000–170.000 g/mol, from ABCR, Germany) or FITC-labeled PAH (PAH-FITC, monomer ratio 50:1 (PAH:FITC), Sigma Aldrich, Germany) in 100 mM NaCl to a concentration of 50 μM, followed by adjusting the pH value to pH 5.4 with NaOH. At this pH value, the weak polyelectrolyte PAH is positively charged, since the isoelectric point of PAH is at pH ~10 (Morga and Adamczyk, 2013).

All synthetic DNA oligonucleotides used in this study were purchased from Biomers (Ulm, Germany): probe ssDNA and FAM-labeled ssDNA (ssDNA-FAM) (52-mer, 5′-TGGAT-CGCTG-TGTAA-GGACA-CGTCG-GCGTG-GTCGT-CTGCT-GGGTT-GATCT-GG-3′); complementary target cDNA and FAM-labeled cDNA (cDNA-FAM) (72-mer, 5′-ACCTC-CGTAA-CCGTC-ATTGT-CCAGA-TCAAC-CCAGC-AGACG-ACCAC-GCCGA-CGTGT-CCTTA-CACAG-CGATC-CA-3′, the complementary part is underlined). Probe DNA-solutions were prepared by dilution of ssDNA or ssDNA-FAM in deionized (DI) water to a final concentration of 5 μM. For the preparation of target cDNA solutions (also 5 μM), cDNA or cDNA-FAM were diluted in 1x PBS (phosphate buffered saline, pH 7.0) adjusted to 0.66 M NaCl. The dsDNA solution was prepared via mixing equal volumes of 5 μM probe ssDNA and 5 μM target cDNA solutions. Before using for surface modification, the dsDNA solution was heated up to 95 °C in a water bath and slowly cooled down to room temperature.

The SG solution has been prepared by 1:1000 dilution of SG stock solution (Sigma Aldrich, Germany) in DI water. The 450 μm thick 3″ boron-doped Si substrates with a crystallographic orientation of < ⟨100⟩ > and a specific electrical resistivity of 1–10 Ωcm were obtained from SiMat (Silicon Materials, Germany).

2.2. EIS-chip fabrication and sensor-surface modification

The capacitive EIS sensor is the simplest electrolyte-gated FED. In contrast to other types of FEDs, like ion-sensitive field-effect transistors or Si-nanowire transistors, capacitive EIS sensors have a simple structure and can be easily fabricated without any photolithographic process steps. The fabrication of the EIS sensor chips used in this work is described in previous literature (Bronder et al., 2015, 2017, 2018). The square-shaped sensor chips (with sizes of 1 cm x 1 cm) consist of an Al/p-Si/SiO_2 structure. The high-quality thermally grown SiO_2 film (thickness: 30 – 50 nm) served as gate insulator. After preparation, the chips were cleaned ultrasonically in a solvent cascade of acetone, isopropyl alcohol, ethanol and DI water, each 3 min. After drying the chips with N_2, they were mounted into a custom-made measurement chamber and sealed with an O-ring (inner diameter: 8 mm) so that a remaining area of approximately 50 mm^2 of SiO_2 surface can get in contact with the solution.

For the surface modification, the biosensor chips were successively exposed to the PAH or particular DNA solution for a time required for the PAH adsorption, ssDNA and dsDNA immobilization or on-chip hybridization of target cDNA, respectively. The SiO_2 gate surface of the EIS chip, which is negatively charged in solutions with pH > pH_{pzc} of ~ 2–2.5 (pzc: point of zero charge) (Poghossian, 1997; van Hal et al., 1996), was modified with positively charged PAH macromolecules by using the well-known layer-by-layer technique (Decher et al., 1998). For this, 100 μL of 50 μM PAH solution was pipetted onto the chip surface and incubated for about 10 min according to the experimental protocol described in (Bronder et al., 2017). The PAH-modified EIS chips were used for the label-free electrostatic detection of ssDNA and in-solution-hybridized dsDNA molecules as well as on-chip hybridization of cDNA with immobilized probe ssDNA (Fig. 1).

For the electrostatic immobilization of negatively charged ssDNA or in-solution-hybridized dsDNA molecules, 100 μL of probe ssDNA or dsDNA solution was applied onto the EIS-sensor surface modified with

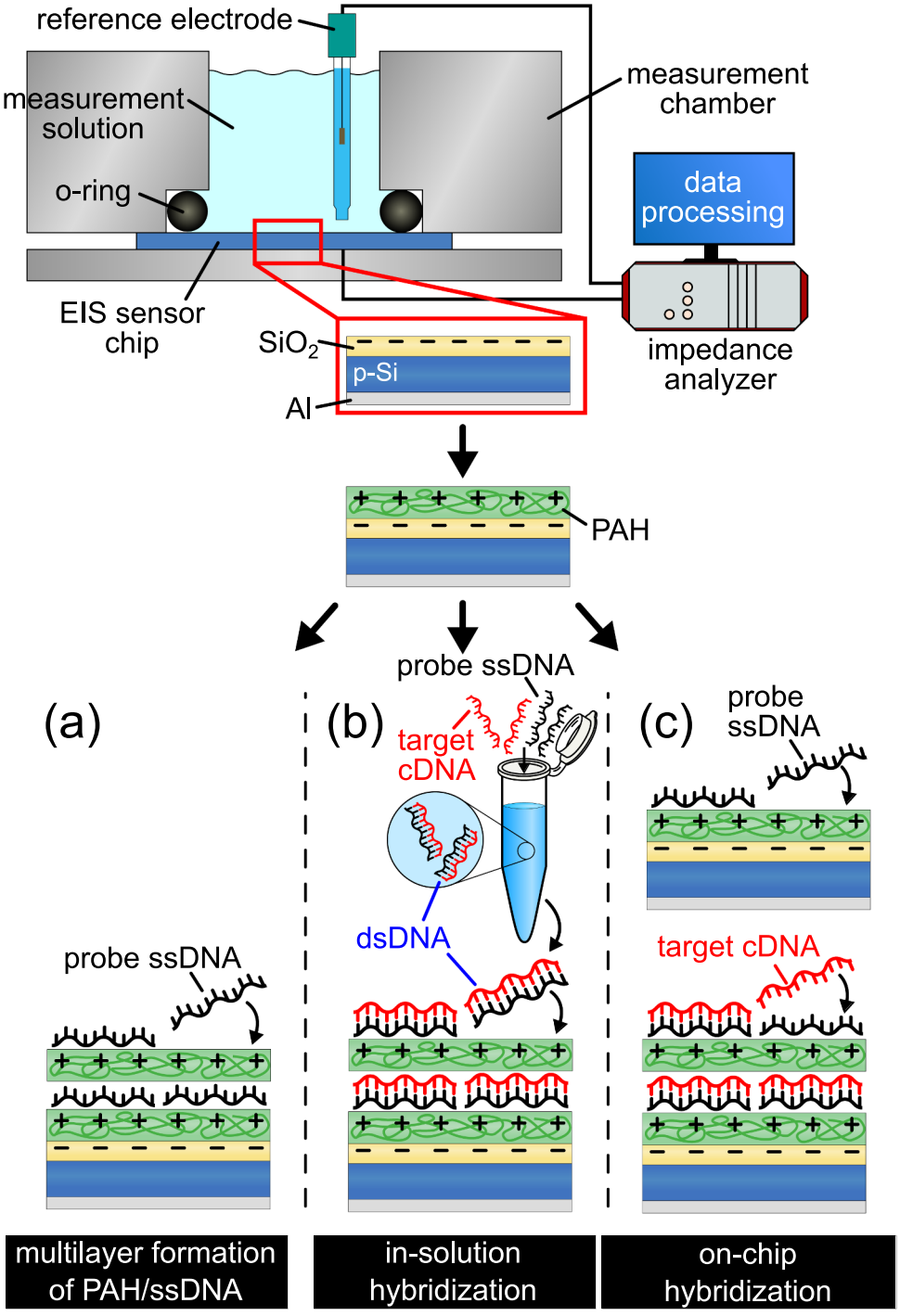

Fig. 1. Cross section of the measurement chamber with an EIS-sensor chip and reference electrode connected to the impedance analyzer for electrochemical characterization. The PAH-modified EIS chips were used for the label-free electrostatic detection of ssDNA (a), in-solution hybridized dsDNA molecules (b) and on-chip hybridization of cDNA with immobilized probe ssDNA (c), respectively.

the positively charged PAH molecules and incubated for 15 min. For the on-chip DNA hybridization, the PAH/ssDNA-modified sensor surface was exposed to 100 µL of 5 µM complementary target cDNA-solution for 40 min. To study the possibility of a multiple surface regeneration and the reusability of the EIS sensors for the DNA detection, the above described procedures were repeated until the desired number of multilayers was achieved (in this work, five layers of PAH/ssDNA, PAH/dsDNA or PAH/ssDNA-cDNA; note that the term ssDNA-cDNA is specified in this work to on-chip hybridized dsDNA in order to distinguish from in-solution hybridized dsDNA). After each surface modification, immobilization and hybridization step, the chip surface was washed with 0.33 mM PBS solution (pH 7.0, ionic strength: 5 mM).

2.3. Electrochemical measurements

The EIS sensor chips have been characterized electrochemically with constant-capacitance (ConCap) method in a two-electrode arrangement using a Zennium impedance analyzer (Zahner Elektrik, Germany). A Ag/AgCl reference electrode (Metrohm, Germany) filled with 3 M KCl was placed into the measurement buffer and connected to

the impedance analyzer. The aluminum rear-side contact of the EIS chip was also connected to the impedance analyzer to close the electrical circuit. For measurements of the sensor response in a dynamic ConCap mode before and after chip-surface modification steps, the capacitance value at/near the inflection point in the depletion region of the capacitance-voltage curve was set constant (Poghossian et al., 2013), while the resulting DC (direct current) voltage, which is required to keep the defined capacitance, was recorded. All ConCap measurements were performed by applying a small superimposed AC voltage (20 mV) with a frequency of 120 Hz. The measurement chamber with the installed sensor chip and reference electrode was filled with the respective solution and placed in a dark Faraday cage to prevent signal-interfering influences from the environment. The pH value of all solutions used in this study was checked before and after each measurement using a pH meter (Mettler Toledo, Germany) with a double-pore pH-glass electrode (Hamilton, Switzerland).

2.4. Optical measurements with fluorescence microscopy

Fluorescence images of the modified biosensor surfaces were taken using an Axio Imager A1m microscope, equipped with a fluorescence filter set (both from Carl Zeiss AG, Germany). The filter set consists of an excitation band-pass filter (455–495 nm), a dichroic beam splitter (500 nm) and an emission band-pass filter (505–555 nm). Fluorescence experiments with three kinds of fluorescence dyes (SG, FITC and FAM) were carried out. These dyes were chosen because their maximum excitation (λ_{ex}) and emission (λ_{em}) wavelengths (SG: λ_{ex} = 498 nm, λ_{em} = 524 nm; FITC: λ_{ex} = 495 nm, λ_{em} = 525 nm and FAM: λ_{ex} = 497 nm, λ_{em} = 525 nm (Xiang et al., 2014; Green, 1990)) fit well to the fluorescence filter set of the microscope used in this experiment. The similarity of the excitation and emission efficiency of the three dyes is beneficial for the data processing and normalization.

For taking fluorescence images from the surface of EIS sensors modified with the in-solution- or on-chip hybridized-dsDNA molecules, they were stained with SG dye. For this, chips were exposed to SG solution for 20 min, washed with 0.33 mM PBS buffer (pH 7.0) and dried with N_2 gas. In case of fluorescence measurements of the chip surfaces modified with PAH-FITC and ssDNA-FAM no additional treatment (fluorescence staining) was needed because these molecules were already labeled with the particular fluorescence dye.

For fluorescence quantification, the respective fluorescence intensity has been determined by the weighted summation of the brightness values from the histogram of the image (Otsu, 1979; Holub and Ferreira, 2006). The histogram data were achieved using ImageJ analysis software.

3. Results and discussion

3.1. Surface regeneration and reusability of PAH-modified EIS sensors for DNA detection

In previous experiments, we demonstrated the feasibility of PAH-modified EIS sensors for the detection of on-chip and in-solution DNA hybridization as well as PCR-amplified DNA fragments (Bronder et al., 2015, 2017, 2018). These were disposable sensors for single measurements. In this work, we studied the possibility of a repeated surface regeneration and the reusability of the PAH-modified EIS sensors for multiple DNA-detection measurements.

At first, the capacitance-voltage curves of bare (unmodified) EIS sensors were recorded in order to check the correct functioning of the chips. Only chips with a (expected) sigmoidal-like shaped curve have been used for further experiments. From the obtained capacitance-voltage signals the working point (i.e., a constant-capacitance value) for subsequent ConCap measurements were chosen.

The ConCap results of reusability experiments are shown in Fig. 2, where three PAH-modified EIS sensors (in total nine EIS sensors were tested) were used for multiple (five times) detection of ssDNA (Fig. 2a), in-solution hybridized dsDNA (Fig. 2b) and on-chip hybridization of complementary target cDNA with an immobilized probe ssDNA (Fig. 2c). The ConCap signals in Fig. 2a-c were recorded in a low ionic-strength buffer solution (0.33 mM PBS, pH 7.0, ionic strength: 5 mM) before and after each surface modification step. After the first successful detection of DNA immobilization or hybridization by the PAH-modified EIS sensors, the surface of all sensors was regenerated by means of simple layer-by-layer adsorption of a second PAH layer on the immobilized ssDNA, dsDNA or on-chip hybridized ssDNA-cDNA layer. Now, the EIS sensors with a positively charged outermost PAH layer are ready for the next electrical DNA-detection measurement. These procedures were repeated five times, demonstrating that via the simple surface regeneration with PAH, the same sensor could be reused for at least five DNA-detection measurements without removal of the underlying layers, which benefits in terms of saving time, effort and costs. The total number of deposited macromolecular layers in experiments shown in Figs. 2a, 2b and 2c was 10, 10 and 15 layers, respectively.

From Fig. 2a–c, it can be clearly recognized that the successive adsorption/immobilization of oppositely charged PAH/ssDNA, PAH/dsDNA and PAH/ssDNA-cDNA layers results in alternate shifting of the ConCap signal. The directions of these signal changes are dependent on the charge sign of the terminating molecular layer. The adsorption of cationic PAH macromolecules shifts the ConCap signal in the direction of more negative voltages. This is due to the feedback control in the ConCap mode, which requires the application of a more negative voltage on the gate for compensation of the positive charge of the PAH molecules and for keeping the EIS capacitance at a constant value. On the contrary, the immobilization of the negatively charged ssDNA, dsDNA and hybridization of cDNA with a probe ssDNA results in a shift of the ConCap response to the direction of less negative gate voltages. Thus, the direction of ConCap-signal shift can serve as an indicator for the verification of successful immobilization or hybridization of DNA molecules. Fig. 2d exemplarily depicts the ConCap-signal changes as a function of the macromolecular layer number evaluated from Fig. 2c for the EIS sensor modified with five $(PAH/ssDNA\text{-}cDNA)_5$ layers. The positively charged PAH layer may attract negatively charged target cDNA molecules and increase their local concentration near the EIS surface as well as may reduce the electrostatic repulsion between probe ssDNA and target cDNA and thus, accelerate the hybridization process even in low ionic-strength solutions. Because of the reversal of the charge sign of the outermost layer after each surface modification with the positively charged PAH layer and subsequent immobilization/hybridization of negatively charged DNA molecules, the signal changes exhibit a zigzag-like behavior. Moreover, the amplitude of the signal changes tends to reduce with an increase of the number of macromolecular layers. For example, signal shifts of 117 mV, 36 mV and 22 mV recorded after the first modification with PAH-1, ssDNA-1 and cDNA-1, respectively, decrease to 14 mV, 10 mV and 3 mV after the fifth modification with PAH-5, ssDNA-5 and cDNA-5 layers. Similar behavior was observed in the case of reusability experiments with EIS sensors for multiple detections of ssDNA and dsDNA shown in Figs. 2a and 2b, respectively. These results are consistent with previous experiments on monitoring of layer-by-layer formation of oppositely charged polyelectrolyte multilayers of PAH/PSS (poly(sodium 4-styrene sulfonate)) using silicon thin-film resistors (Neff et al., 2006, 2007) and capacitive field-effect sensors (Poghossian et al., 2013). On the other hand, no signal reducing with increasing the layer number was observed for an EIS sensor modified with poly-L-lysine/DNA multilayer in other studies (Fritz et al., 2002; Hou et al., 2006) that could be probably due to, for instance, a highly porous multilayer structure.

To explain gate-surface potential changes of capacitive EIS sensors induced via layer-by-layer adsorption of polyelectrolytes, a theoretical electrostatic model has been developed in (Poghossian et al., 2013). This model takes into account the ionic strength of the solution and the screening of macromolecular charge by the counter ions as well as the

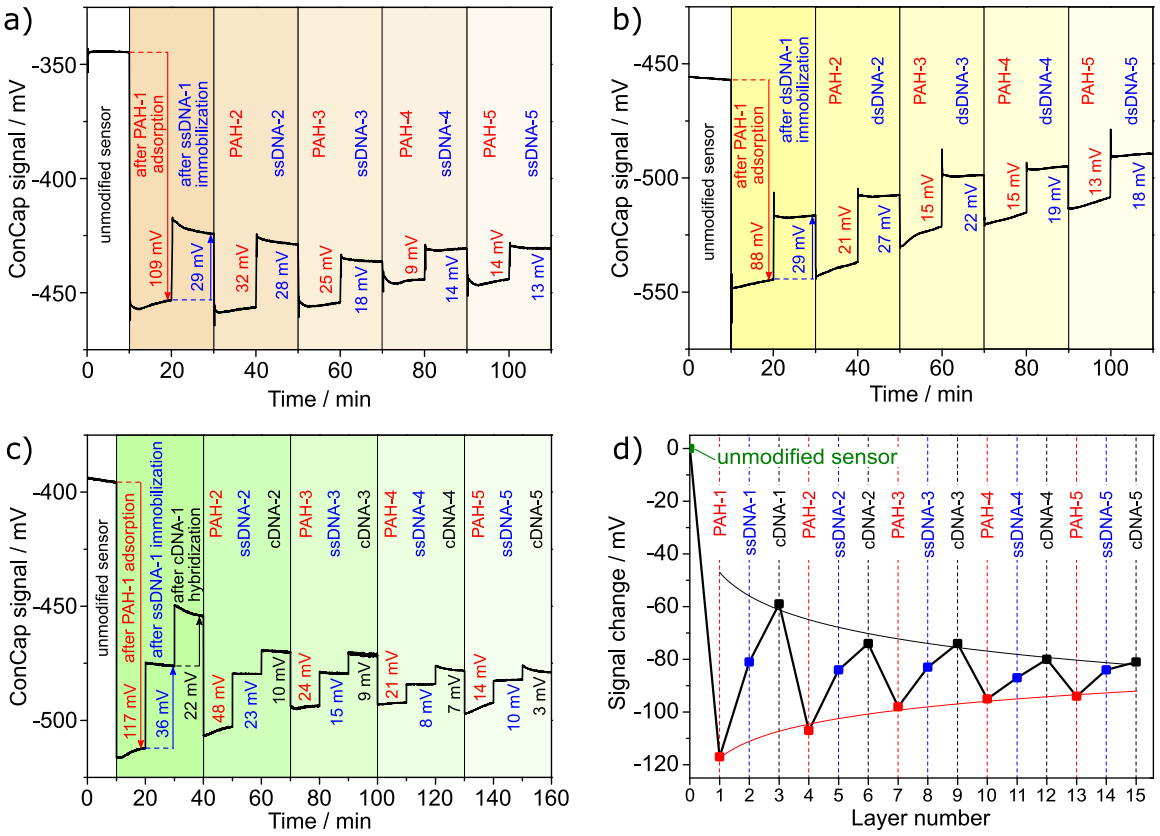

Fig. 2. ConCap curves of EIS sensors modified with PAH/ssDNA (a), PAH/dsDNA (b), PAH/ssDNA-cDNA (c) multilayers and signal changes as a function of layer number (d), evaluated from (c).

distance between the charge of the terminating polyelectrolyte layer and the sensor surface. Although this model was developed for EIS sensors modified with a multilayer of oppositely charged PAH/PSS, it can also be applied to qualitatively explain the signal behavior of the EIS sensor modified with the multilayer of the PAH/DNA system. The model predicts the decreasing of signal changes upon subsequent adsorption of oppositely charged polyelectrolytes as the ionic strength of the solution increased, because of a more efficient screening of the polyelectrolyte charge (the experimental results related to this issue are presented in Subsection 3.2: Influence of ionic strength on the sensor signal). The model also predicts reducing of the electrostatic interaction between the charged polyelectrolyte and the EIS gate surface with increasing the distance between the terminating molecular layer and the gate surface. Thus, the signal changes generated due to the PAH adsorption or DNA immobilization/hybridization will reduce with the rise of the layer number and thickness of PAH/DNA multilayer that in fact, has been monitored in our experiments.

3.2. Influence of ionic strength on the sensor signal

The charge distribution in the immediate vicinity of the gate surface plays a critical role in transferring the molecular charge-induced signal to the EIS device. EIS sensors are known as charge-sensitive devices (Bergveld, 1991; Poghossian et al., 2007); they are able to detect charge changes that happen directly at the gate surface or within the order of the Debye length (λ_D) from the surface. Therefore, the Debye-screening length is obviously one of the important factors, which may significantly affect the working characteristics (output-signal change, sensitivity, detection limit, etc.) of FEDs for the detection of adsorption/binding of charged macromolecules onto the gate surface (Liu and Dutton, 2009; Chen et al., 2011; Stern et al., 2007). The charge of the macromolecules is screened by the dissolved small counterions in the solution: positively charged macromolecules such as PAH will be surrounded by anions due to electrostatic interactions, while negatively charged species such as DNA will be surrounded by cations. As a result of the charge-screening effect, the electrostatic potential arising from the intrinsic charges of molecules decays exponentially with distance to nearly zero in the bulk-electrolyte solution. The Debye length is the distance over which the electrostatic potential decreases by a factor of e (~2.7). It is inversely proportional to the ionic strength of the electrolyte solution and for aqueous solutions is given by Eq. (1) (Poghossian et al., 2005; Goda et al., 2013):

$$\lambda_D = \sqrt{\frac{\varepsilon_0 \varepsilon_r k_B T}{2 z^2 q^2 I_s}} \quad (1)$$

where ε_r is the dielectric constant of the electrolyte solution, ε_0 is the vacuum permittivity, k_B is the Boltzmann constant, T is the temperature, z is the valency of the ions in the electrolyte, q is the elementary charge, and I_s is the ionic strength of the electrolyte, which for a 1:1 monovalent salt can be replaced by the ion concentration. For a monovalent electrolyte at 25 °C the Debye length can be simply determined from Eq. (2):

$$\lambda_D \,(\text{in nm}) \approx \frac{0.304}{\sqrt{I_s}} \,(inM) \quad (2)$$

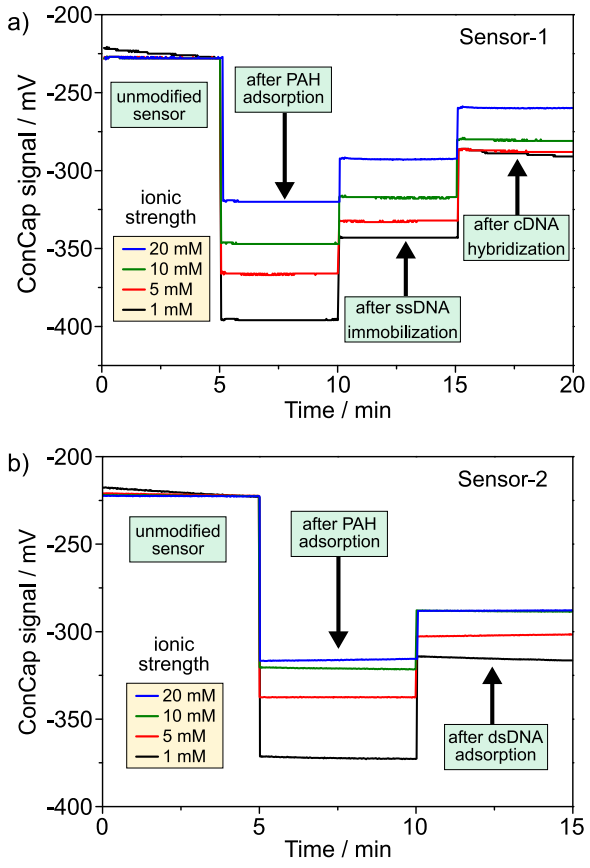

Fig. 3. ConCap signal of two EIS biosensors recorded in 0.066 mM, 0.33 mM, 0.66 mM and 1.32 mM PBS solutions (pH 7.0) with different ionic strength of 1 mM, 5 mM, 10 mM and 20 mM, respectively. a) Sensor-1: before and after PAH adsorption, immobilization of probe ssDNA and on-chip hybridization of target cDNA molecules; b) Sensor-2: before and after PAH adsorption and dsDNA immobilization.

Table 1
ConCap-signal changes after each surface-modification step recorded in PBS solutions with different ionic strength.

		Sensor signal change / mV				
		Sensor-1 on-chip hybridization			Sensor-2 in-solution hybridization	
Ionic strength / mM	Debye length / nm	After PAH	After ssDNA	After cDNA	After PAH	After dsDNA
1	9.6	167	53	52	151	56
5	4.3	138	34	44	115	36
10	3.0	119	30	36	98	33
20	2.2	92	27	33	92	27

To find out an influence of the ionic strength, the ConCap-signal changes induced by the each surface-modification step (i.e., after PAH adsorption, immobilization of ssDNA and dsDNA molecules and after on-chip hybridization of cDNA) were recorded in PBS solutions (pH 7.0) with different ionic strength of 1 mM, 5 mM, 10 mM and 20 mM (the corresponding Debye lengths amount approximately 9.6 nm, 4.3 nm, 3 nm and 2.2 nm, respectively). The results of these experiments are depicted in Fig. 3.

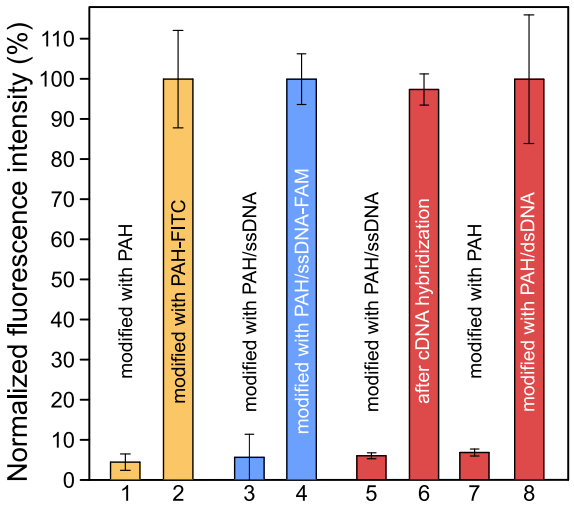

Fig. 4. Bar chart of the normalized average fluorescence intensities of fluorescence images taken from the gate surfaces of EIS sensors after various modification steps by using fluorescence dyes of FITC (bar 1, 2), FAM (bar 3, 4) and SG (bar 5–8), respectively. The fluorescence signals were normalized for each fluorescence dye individually by setting the highest recorded value to 100%.

The ConCap-signal changes after each modification step evaluated from Fig. 3 are summarized in Table 1. As expected, with increasing the ionic strength of the solution, the amplitude of signal shifts after each modification step is decreased. This is due to the more efficient screening of the molecular charge of PAH or DNA by counter ions in the solution. For example, the on-chip cDNA-hybridization signal is reduced from 52 mV recorded in PBS with ionic strength of 1 mM to 33 mV measured in PBS with ionic strength of 20 mM.

3.3. Fluorescence-intensity measurements of modified sensor surfaces

To verify the results of field-effect experiments, fluorimetric investigations were performed by using the fluorescence dyes FITC, FAM and SG. Fig. 4 shows a colored bar chart representing the normalized average fluorescence intensities of fluorescence images taken from the gate surfaces of the EIS sensors after various modification steps (in total 24 sensor chips were studied). The two orange-colored bars (1–2) represent the fluorescence signals for a SiO_2-gate surface modified with PAH or PAH-FITC, respectively. PAH molecules bind to the sensor surface in both cases, but a strong fluorescence only occurs for the PAH-FITC-modified chip because of the presence of the fluorescence dye.

In order to proof an immobilization of ssDNA onto the PAH layer, additional reference experiments were carried out utilizing FAM-labeled ssDNA molecules. The fluorescence signals of two chip surfaces, which were modified with PAH/ssDNA and PAH/ssDNA-FAM (blue bars 3–4), were compared. As expected, a significant increase in fluorescence intensity has been detected from the chip surface modified with PAH/ssDNA-FAM. This experiment confirms the successful electrostatic immobilization of the negatively-charged probe ssDNA-molecules onto the PAH-modified SiO_2 surface.

Finally, the red bars (5–8) in Fig. 4 represent the results of fluorescent experiments in which SG was used as fluorescence dye. For this purpose, two EIS sensors modified with the in-solution (bar 8) or on-chip hybridized dsDNA molecules (bar 6) were incubated in SG solution. For comparison, two other EIS sensors modified with PAH or PAH/ssDNA layers (i.e., without in-solution- or on-chip-hybridized dsDNA) were also exposed to SG solution. SG dye is known for the strong

brightness increase upon binding to dsDNA (Xiang et al., 2014). As can be seen, fluorescence intensities of less than 8% (bars 5 and 7) were detected for EIS sensors modified with PAH or PAH/ssDNA layers, because no dsDNA is present on the sensor surface. In contrast, fluorescence intensity of approximately 100% was observed for the EIS sensor modified with PAH/ssDNA layers and exposed to target cDNA solution (bar 6). This result indicates the successful hybridization of the target cDNA molecules with the immobilized probe ssDNA and formation of dsDNA. A high fluorescence intensity of ~100% was also observed when in-solution-hybridized dsDNA molecules were directly immobilized onto the PAH-modified surface (bar 8). In both cases, SG binds to dsDNA molecules, resulting in a strong increase of brightness. Thus, the results of fluorescence-intensity measurements correlate well with the results obtained by field-effect experiments and validate successfully all surface-modification steps.

4. Conclusions

In this work, the reusability of PAH-modified capacitive field-effect EIS sensors for the label-free electrical detection of ssDNA, in-solution- and on-chip-hybridized dsDNA has been investigated. For this, the formation of five bilayers of PAH/ssDNA or PAH/dsDNA as well as five triple layers of PAH/ssDNA-cDNA onto the EIS gate surface was monitored by means of dynamic ConCap measurements. It has been demonstrated that via simple regeneration of the EIS-sensor surface by means of adsorption of a new PAH layer, the same biosensor could be reused for at least five DNA-detection measurements. The consecutive adsorption of oppositely charged PAH/ssDNA, PAH/dsDNA and PAH/ssDNA-cDNA layers leads to alternating shifts of the ConCap signal. The direction of the EIS-signal shifts depends on the charge sign of the outermost molecular layer and therefore, can be used as an indicator for the verification of successful DNA-immobilization or hybridization processes.

In addition, an influence of the Debye-screening effect (which is considered as one of the important factors affecting the sensitivity of FEDs to the macromolecular charge) on the EIS signal has been studied by recording ConCap responses after each surface-modification steps in buffer solutions with different ionic strength. The ConCap-signal changes induced by each modification step (i.e., PAH adsorption, immobilization of ssDNA or dsDNA molecules and on-chip hybridization of cDNA) is increased with decreasing the ionic strength of the solution, due to the less efficient screening of the molecular charge of the PAH or DNA by counterions. The results of field-effect measurements were supported by fluorescence-microscopy experiments using PAH and ssDNA molecules labeled with fluorescence dyes of FITC and FAM, respectively, as well as via staining of the in-solution- and on-chip-hybridized dsDNA with SG dye.

It is worth to note, although in this work, a multilayer PAH/DNA system has been studied, the capacitive EIS platform can be extended for the label-free electrical monitoring of formation of multilayers composed of other oppositely charged cationic/anionic macromolecular systems as well as charged nanoparticle/molecule inorganic/organic nanohybrids.

Acknowledgements

The authors thank S. Scheja for technical support, H. Iken for wafer processing and C. Metzger-Boddien, H. Busch for valuable discussions. The authors wish to acknowledge the German Federal Ministry of Education and Research for the financial support (project “DiaCharge”, grant no.: 031A192D), Germany.

Declarations of interest

The authors declare no competing financial interest.

References

Bandiera, L., Cellere, G., Cagnin, S., Toni, A., Zanoni, E., Lanfranchi, G., Lorenzelli, L., 2007. Biosens. Bioelectron. 22, 2108–2114.
Bergveld, P., 1991. Biosens. Bioelectron. 6, 55–72.
Braeken, D., Reekmans, G., Zhou, C., van Meerbergen, B., Callewaert, G., Borghs, G., Bartic, C., 2008. J. Exp. Nanosci. 3, 157–169.
Bronder, T.S., Poghossian, A., Scheja, S., Wu, C., Keusgen, M., Mewes, D., Schöning, M.J., 2015. ACS Appl. Mater. Interfaces 7, 20068–20075.
Bronder, T.S., Poghossian, A., Keusgen, M., Schöning, M.J., 2017. Tech. Mess. 84, 628–634.
Bronder, T.S., Jessing, M.P., Poghossian, A., Keusgen, M., Schöning, M.J., 2018. Anal. Chem. 90, 7747–7753.
Chen, K.I., Li, B.R., Chen, Y.T., 2011. Nano Today 6, 131–154.
Credo, G.M., Su, X., Wu, K., Elibol, O.H., Liu, D.J., Reddy, B., Tsai, T.W., Dorvel, B.R., Daniels, J.S., Bashir, R., Varma, M., 2012. Analyst 137, 1351–1362.
Decher, G., Eckle, M., Schmitt, J., Struth, B., 1998. Curr. Opin. Colloid Interface Sci. 3, 32–39.
Evtugyn, G.A., Hianik, T., 2011. Curr. Anal. Chem. 7, 8–34.
Fritz, J., Cooper, E.B., Gaudet, S., Sorger, P.K., Manalis, S.R., 2002. Proc. Natl. Acad. Sci. USA 99, 14142–14146.
Goda, T., Singi, A.B., Maeda, Y., Matsumoto, A., Torimura, M., Aoki, H., Miyahara, Y., 2013. Sensors 13, 2267–2278.
Goda, T., Tabat, M., Miyahara, Y., 2015. Bioeng. Biotechnol. 3, 1–7.
Goode, J.A., Rushworth, J.V.H., Millner, P.A., 2015. Langmuir 31, 6267–6276.
Green, F.J., 1990. The Sigma-Aldrich Handbook of Stains, Dyes, and Indicators. Aldrich Chemical Co., Milwaukee.
Gun, J., Schöning, M.J., Abouzar, M.H., Poghossian, A., Katz, E., 2008. Electroanalysis 20, 1748–1753.
Holub, O., Ferreira, S.T., 2006. Comput. Phys. Commun. 175, 620–623.
Hou, C.S.J., Milovic, N., Godin, M., Russo, P.R., Chakrabarti, R., Manalis, S.R., 2006. Anal. Chem. 78, 2526–2531.
Hou, C.S.J., Godin, M., Payer, K., Chakrabarti, R., Manalis, S.R., 2007. Lab Chip 7, 347–354.
Ingebrandt, S., Offenhäusser, A., 2006. Phys. Status Solidi A 203, 3399–3411.
Ingebrandt, S., Han, Y., Nakamura, F., Poghossian, A., Schöning, M.J., Offenhäusser, A., 2007. Biosens. Bioelectron. 22, 2834–2840.
Jimenez-Jorquera, C., Orozco, J., Baldi, A., 2010. Sensors 10, 61–83.
Kamahori, M., Ishige, Y., Shimoda, M., 2008. Biosens. Bioelectron. 23, 1046–1054.
Kataoka-Hamai, C., Miyahara, Y., 2011. IEEE Sens. J. 11, 3153–3160.
Lai, S., Barbaro, M., Bonfiglio, A., 2015. Appl. Phys. Lett. 107, 103301.
Lee, C.S., Kim, S.K., Kim, M., 2009. Sensors 9, 7111–7131.
Lin, T.W., Kekuda, D., Chu, C.W., 2010. Biosens. Bioelectron. 25, 2706–2710.
Liu, Y., Dutton, R.W., 2009. J. Appl. Phys. 106, 14701.
Lu, N., Gao, A., Dai, P., Li, T., Wang, Y., Gao, X., Song, S., Fan, C., Wang, Y., 2013. Methods 63, 212–218.
Morga, M., Adamczyk, Z., 2013. J. Colloid Interface Sci. 407, 196–204.
Nakazato, K., 2009. Sensors 9, 8831–8851.
Neff, P.A., Naji, A., Ecker, C., Nickel, B., Klitzing, R., Bausch, A.R., 2006. Macromolecules 39, 463–466.
Neff, P.A., Wunderlich, B.K., Klitzing, R., Bausch, A.R., 2007. Langmuir 23, 4048–4052.
Nishio, Y., Uno, S., Nakazato, K., 2013. Jpn. J. Appl. Phys. 52, 04CL01.
Otsu, N., 1979. IEEE T. Syst. Man. Cybern. 9, 62–66.
Poghossian, A., 1997. Sens. Actuators B 44, 551–553.
Poghossian, A., Schöning, M.J., 2014. Electroanalysis 26, 1197–1213.
Poghossian, A., Thust, M., Schöning, M.J., Müller-Veggian, M., Kordos, P., Lüth, H., 2000. Sens. Actuators B 68, 260–265.
Poghossian, A., Baade, A., Emons, H., Schöning, M.J., 2001. Sens. Actuators B 76, 634–638.
Poghossian, A., Cherstvy, A., Ingebrandt, S., Offenhäusser, A., Schöning, M.J., 2005. Sens. Actuators B 111–112, 470–480.
Poghossian, A., Ingebrandt, S., Abouzar, M.H., Schöning, M.J., 2007. Appl. Phys. A 87, 517–524.
Poghossian, A., Weil, M., Cherstvy, A.G., Schöning, M.J., 2013. Anal. Bioanal. Chem. 405, 6425–6436.
Poghossian, A., Bäcker, M., Mayer, D., Schöning, M.J., 2015. Nanoscale 7, 1023–1031.
Poghossian, A., Bronder, T.S., Scheja, S., Wu, C., Weinand, T., Metzger-Boddien, C., Keusgen, M., Schöning, M.J., 2016. Procedia Eng. 168, 514–517.
Purushothaman, S., Toumazou, C., Ou, C., 2006. Sens. Actuators B 114, 964–968.
Rothberg, J.M., Hinz, W., Rearick, T.M., Schultz, J., Mileski, W., Davey, M., Leamon, J.H., Johnson, K., Milgrew, M.J., Edwards, M., Hoon, J., Simons, J.F., Marran, D., Myers, J.W., Davidson, J.F., Branting, A., Nobile, J.R., Puc, B.P., Light, D., Clark, T.A., Huber, M., Branciforte, J.T., Stoner, I.B., Cawley, S.E., Lyons, M., Fu, Y., Homer, N., Sedova, M., Miao, X., Reed, B., Sabina, J., Feierstein, E., Schorn, M., Alanjary, M., Dimalanta, E., Dressman, D., Kasinskas, R., Sokolsky, T., Fidanza, J.A., Namsaraev,

E., McKernan, K.J., Williams, A., Roth, G.T., Bustillo, J., 2011. Nature 475, 348–352.
Salm, E., Zhong, Y., Reddy, B., Duarte-Guevara, C., Swaminathan, V., Liu, Y.S., Bashir, R., 2014. Anal. Chem. 86, 6968–6975.
Sassolas, A., Leca-Bouvier, B.D., Blum, L.J., 2008. Chem. Rev. 108, 109–139.
Siqueira, J.R., Abouzar, M.H., Bäcker, M., Zucolotto, V., Poghossian, A., Oliveira, O.N., Schöning, M.J., 2009. Phys. Status Solidi A 206, 462–467.
Stern, E., Wagner, R., Sigworth, F.J., Breaker, R., Fahmy, T.M., Reed, M.A., 2007. Nano Lett. 7, 3405–3409.
Toumazou, C., Shepherd, L.M., Reed, S.C., Chen, G.I., Patel, A., Garner, D.M., Wang, C.J.A., Ou, C.P., Amin-Desai, K., Athanasiou, P., Bai, H., Brizido, I.M., Caldwell, B., Coomber-Alford, D., Georgiou, P., Jordan, K.S., Joyce, J.C., La Mura, M., Morley, D., Sathyavruthan, S., Temelso, S., Thomas, R.E., Zhang, L., 2013. Nat. Methods 10, 641–646.
Toumazou, C., Thay, T.S.L.K., Georgiou, P., 2014. Philos. Trans. R. Soc. A 372, 20130112.
van Hal, R.E.G., Eijkel, J.C.T., Bergveld, P., 1996. Adv. Colloid Interface Sci. 69, 31–62.
Veigas, B., Branquinho, R., Pinto, J.V., Wojcik, P.J., Martins, R., Fortunato, E., Baptista, P.V., 2014. Biosens. Bioelectron. 52, 50–55.
Veigas, B., Fortunato, E., Baptista, P.V., 2015. Sensors 15, 10380–10398.
Wei, F., Lillehoj, P.B., Ho, C.M., 2010. Pediatr. Res. 67, 458–468.
Wu, C., Bronder, T., Poghossian, A., Werner, C.F., Bäcker, M., Schöning, M.J., 2014. Phys. Status Solidi A 211, 1423–1428.
Wu, C., Poghossian, A., Bronder, T.S., Schöning, M.J., 2016. Sens. Actuators B 229, 506–512.
Wu, C.S., Bronder, T., Poghossian, A., Werner, C.F., Schöning, M.J., 2015. Nanoscale 7, 6143–6150.
Xiang, D., Zhai, K., Xiang, W., Wang, L., 2014. Talanta 129, 249–253.
Zhang, G.J., Zhang, G., Chua, J.H., Chee, R.E., Wong, E.H., Agarwal, A., Buddharaju, K.D., Singh, N., Gao, Z.Q., Balasubramanian, N., 2008. Nano Lett. 8, 1066–1070.
Zhao, W.W., Xu, J.J., Chen, H.Y., 2014. Chem. Rev. 114, 7421–7441.